Supporting Information

Synthesis of porous NiO/CeO_2 hybrid nanoflake arrays as platform for electrochemical biosensing

Jiewu Cui*[a,b], Jinbao Luo[a], Bangguo Peng[a,b], Xinyi Zhang*[b], Yong Zhang[a,b], Yan Wang[a,b], Yongqiang Qin[a], Hongmei Zheng[a], Xia Shu[a,b] and Yucheng Wu*[a,b]

[a] School of Materials Science and Engineering, Hefei University of Technology, Hefei, 230009, China

[b] Key Laboratory of Advanced Functional Materials and Devices of Anhui Province, Hefei, 230009, China

Author to whom any correspondence should be addressed, e-mail: ycwu@hfut.edu.cn, Fax:+86-551-62904517, Tel: +86-551-62901012

Experimental details

Materials synthesis:

Porous NiO/CeO_2 nanoflake arrays (NFAs) were fabricated by hydrothermal method on Ni foam. Prior to synthesis of NiO/CeO_2 NFAs, Ni foam (2 cm×3 cm) was rinsed with ethanol and Milli-Q water (18.25 MΩ·cm) alternatively. And then it was immersed into 3 M HCl overnight to remove the surface oxide layer. To synthesize the NiO/CeO_2 NFAs, 35 mL mixture solution with different concentrations of $Ce(NO_3)_3$, NH_4F and $CO(NH)_2$ was prepared and subsequently transferred to a 50 mL Teflon vessel with an autoclavable screw cap. The pre-treated Ni foam was immersed into the 35 mL mixture solution. Afterwards, the autoclave was heated to different temperatures for different time inside a conventional oven. The samples were washed repeatedly with Milli-Q water and annealed at 500℃ for 2h in air. The influence of $Ce(NO_3)_3$, NH_4F and $CO(NH)_2$ concentrations, temperature and time of hydrothermal process on the morphology of the products was investigated and discussed in detail in this communication.

Materials Characterization:

The as-prepared samples were characterized by field emission scanning electron microscopy (SU8020, Hitachi, Japan), X-ray diffraction (D/MAX2500V, Rigaku, Japan), transmission electron microscopy (JEM-2100F, JEOL, Japan). X-ray photoelectron spectrum (ESCALAB250, Thermo, US) was also employed to analyze the elemental status of the NiO/CeO_2 NFAs.

Fabrication of glucose biosensor and electrochemical measurements

Glucose biosensor was fabricated according to our previously reported method [1]. Typically, 50 μL mixture solution with 4.5 v/v% glutaraldehyde, 4.8 w/v% bovine serum albumin and 200 U/mL glucose oxidase was freshly prepared, subsequently a slice of Ni foam (geometry area: 0.1 cm^2) with porous NiO/CeO_2 NFAs was immersed into the mixture solution and dried in air for 2 h.

Cyclic voltammograms, electrochemical impedance spectrum and chronoamperometry were carried out on autolab PGSTAT 302N electrochemical workstation with a conventional three electrode system. Enzyme modified porous NiO/CeO_2 NFAs on Ni foam, Ag/AgCl (3M KCl) and Pt/Ti were used as working electrode, reference electrode and counter electrode, respectively.

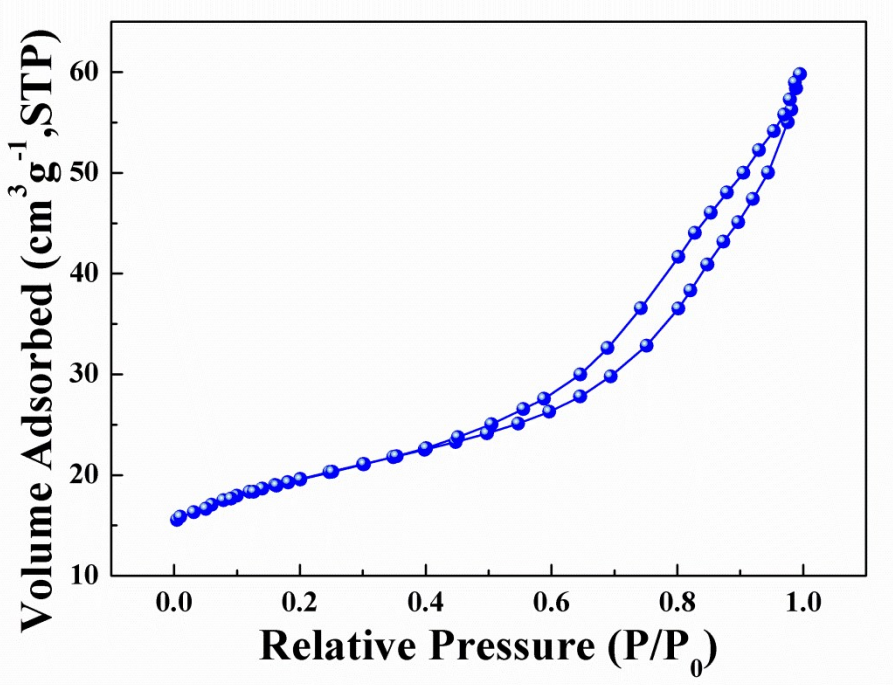

Fig. S1 N_2 adsorption and desorption isotherm of NiO/CeO_2 hybrid nanoflake arrays

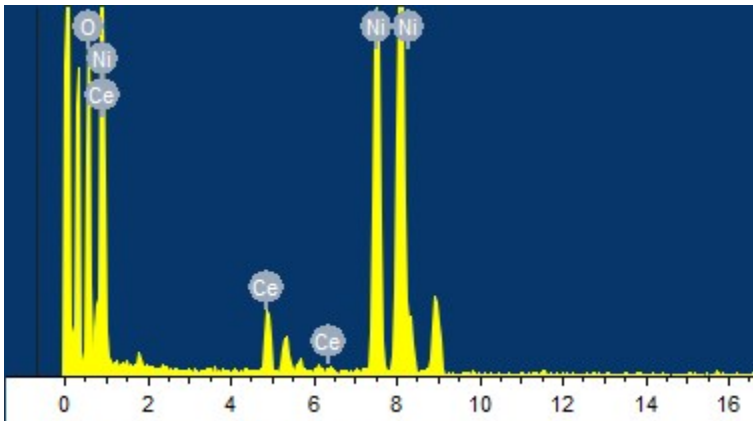

Fig. S2 EDS analysis of an individual NiO/CeO_2 hybrid nanoflake

Table S1 Elemental composition in an individual NiO/CeO_2 hybrid nanoflake

Element	Weight percentage	Atomic percentage
O K	26.65	61.57
Ni K	52.16	32.84
Ce L	21.19	5.59
Total	100.00	

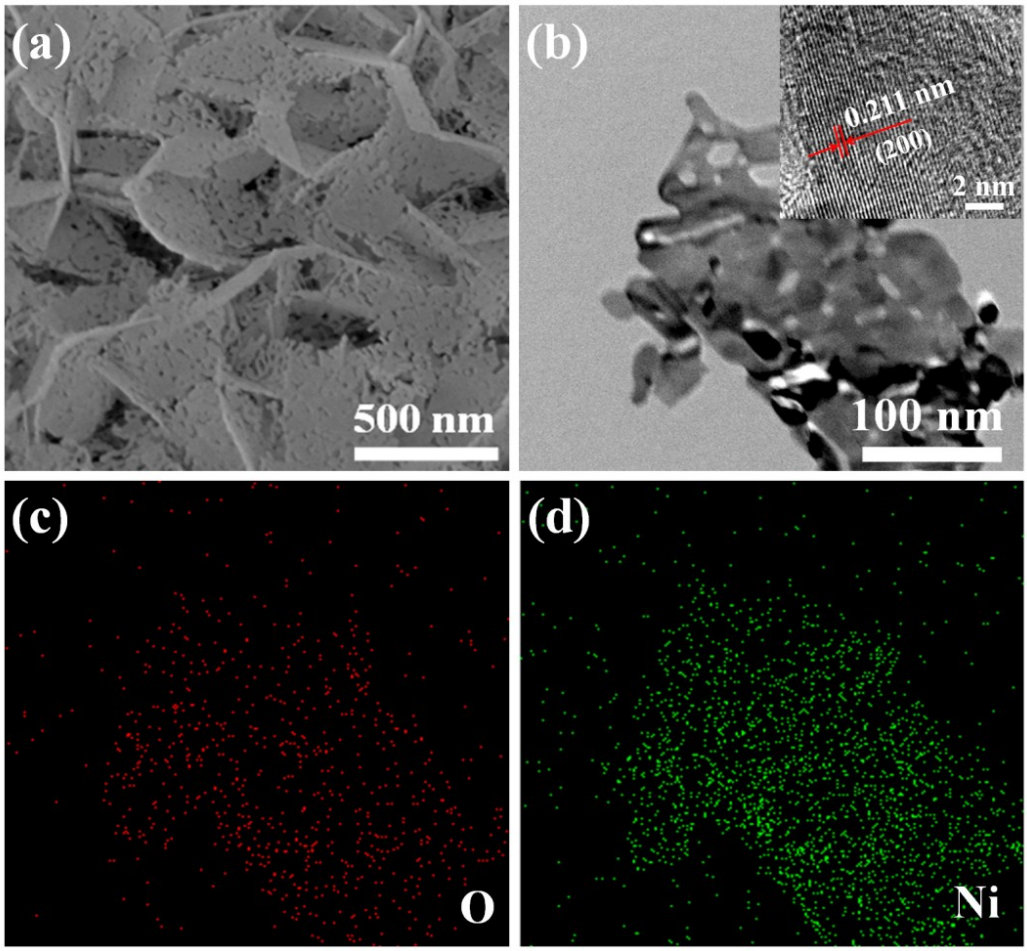

Fig. S3 (a) SEM image of NiO nanoflake arrays. (b) TEM image of a single NiO nanoflake, inset is the HRTEM image of corresponding single NiO nanoflake. Elemental distribution of O (c) and Ni (d) in a single NiO nanoflake in Fig. S3 (b).

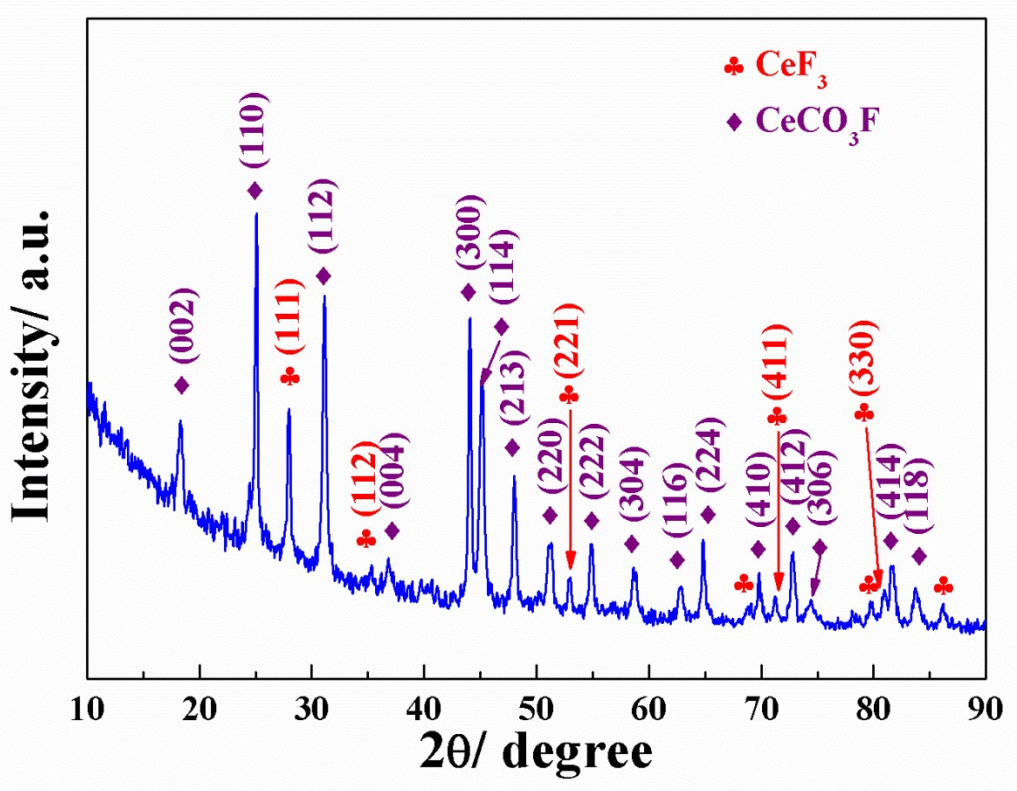

Fig. S4 XRD pattern of samples prepared by hydrothermal method in solution containing $Ce(NO_3)_3$, NH_4F and $CO(NH)_2$ without nickel foam

Fig. S4 shows XRD pattern of samples prepared by the same hydrothermal method in solution containing $Ce(NO_3)_3$, NH_4F and $CO(NH)_2$ without nickel foam. The result indicates that the products are CeF_3 and $CeCO_3F$, which are totally different from the precursors ($Ni(OH)_2$ and $Ce(OH)_3$) synthesized on the nickel foam.

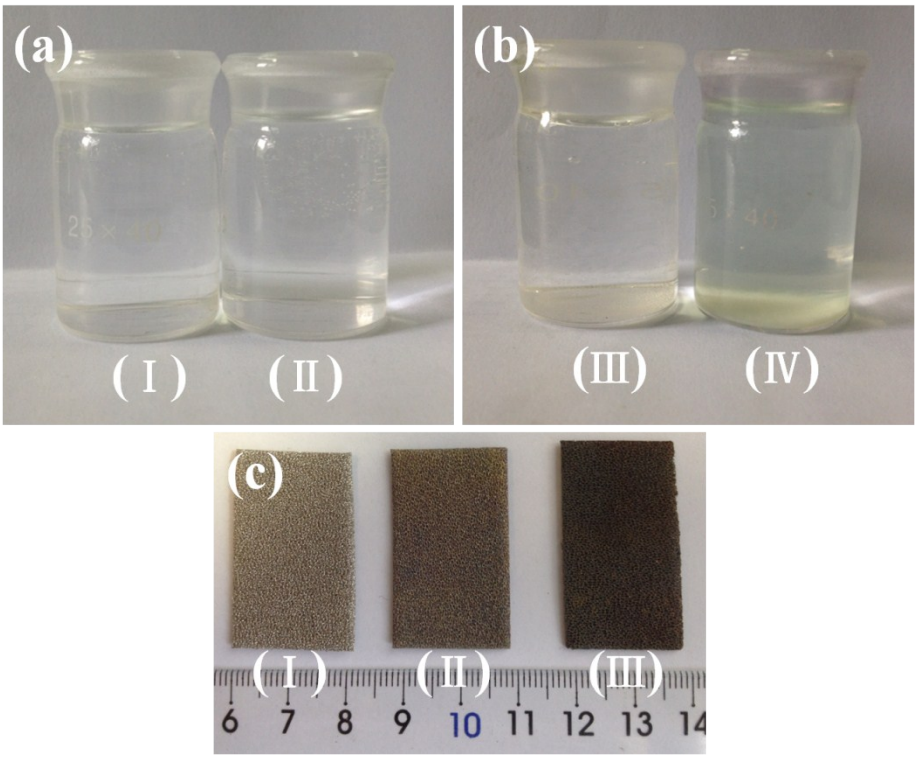

Fig. S5 (a) Reaction solutions contain NH_4F and $CO(NH)_2$ before (I) and after (Ⅱ) hydrothermal reaction. (b) Reaction solutions contain $Ce(NO_3)_3$, NH_4F and $CO(NH)_2$ before (I) and after (Ⅱ) hydrothermal reaction. (c) Nickel foam (I), Nickel foam with samples before (Ⅱ)and after (Ⅲ) calcinations.

Fig. S5 (a) demonstrates the colour change of hydrothermal reaction solutions only contain NH_4F and $CO(NH)_2$ before (I) and after (Ⅱ) hydrothermal reaction. It is apparent that the colour of hydrothermal reaction solution is still transparent and the same as that before hydrothermal reaction. However, the colour of solutions changes into pale green (as shown in Fig. S5(b)) after hydrothermal reaction with $Ce(NO_3)_3$ in the reaction solution. And the reason for this phenomenon will be explained in the following section. Fig. S5 (c) presents the Nickel foam (I), Nickel foam with samples before (Ⅱ)and after (Ⅲ) calcinations, the real samples show different colours at different stage, indicating the successful synthesis of expected NiO/CeO_2 hybrid nanoflake arrays.

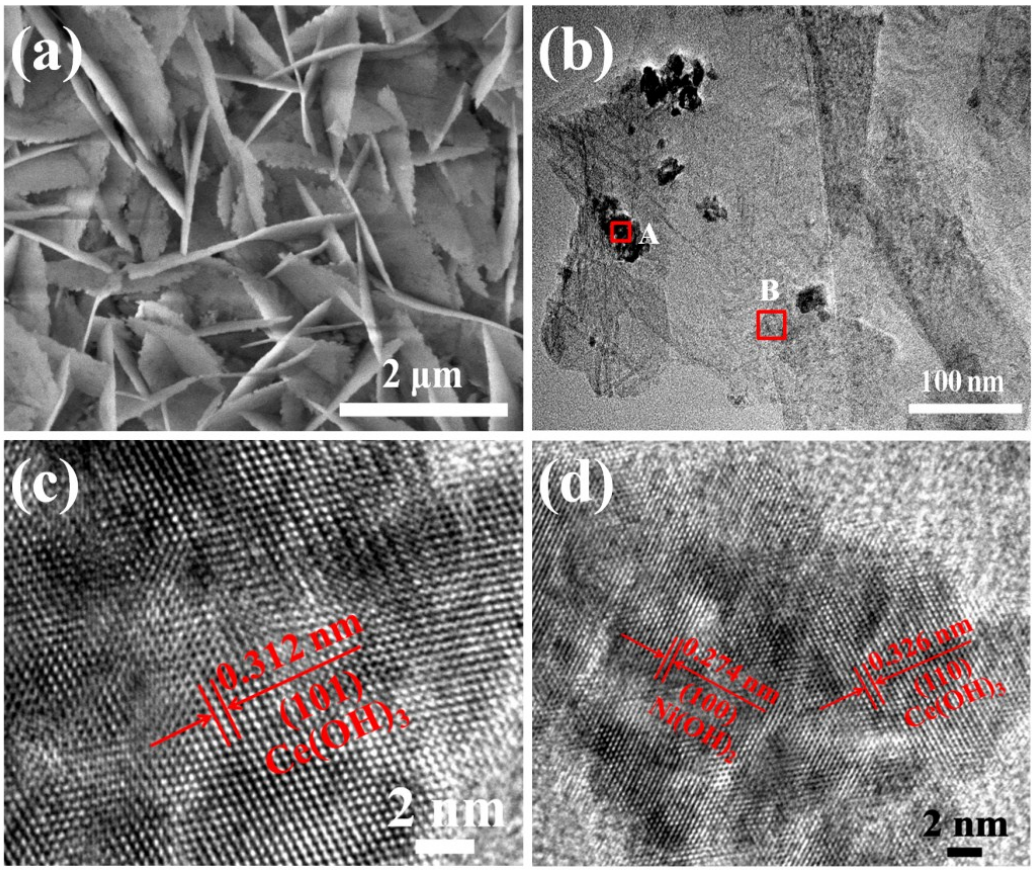

Fig. S6 (a) SEM image of $Ni(OH)_2/Ce(OH)_3$ hybrid NFAs. (b) TEM image of a single $Ni(OH)_2/Ce(OH)_3$ hybrid nanoflake. (c) and (d) are HRTEM images at spots (A) and (B) in Fig. S5(b), respectively.

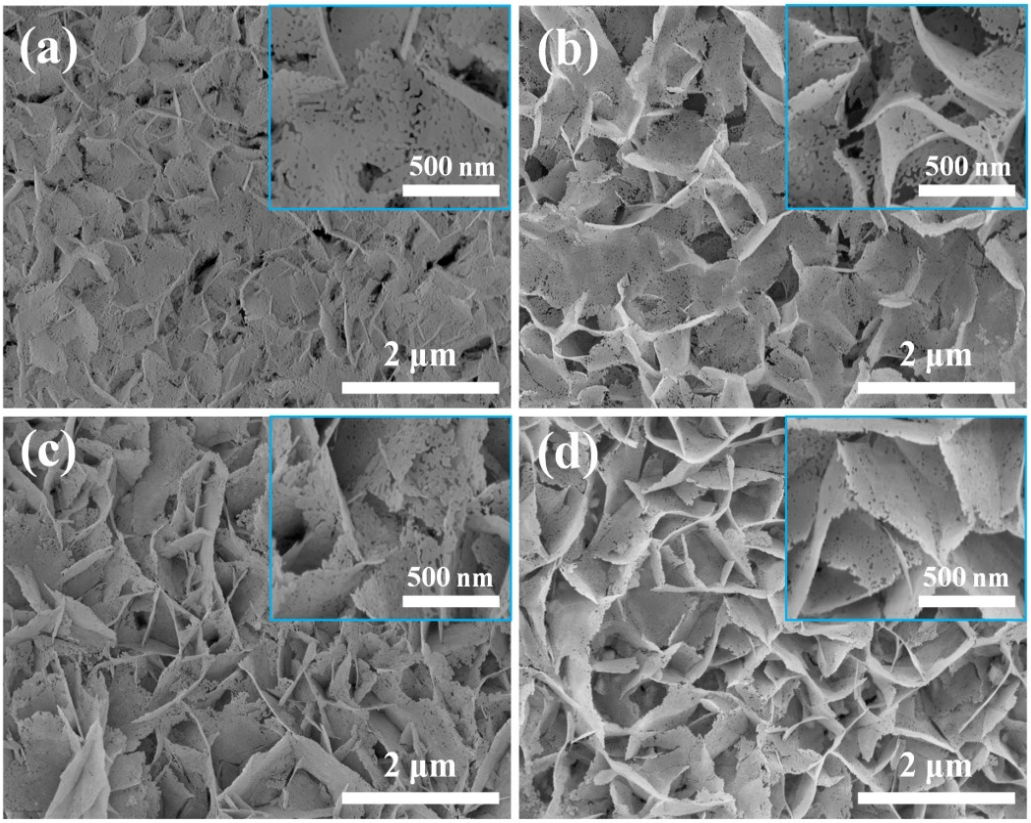

Fig. S7 Influence of $Ce(NO_3)_3$ concentration on the morphology of NiO/CeO_2 hybrid NFAs. (a) 0, (b) 5 mM, (c) 10 mM and (d) 15 mM.

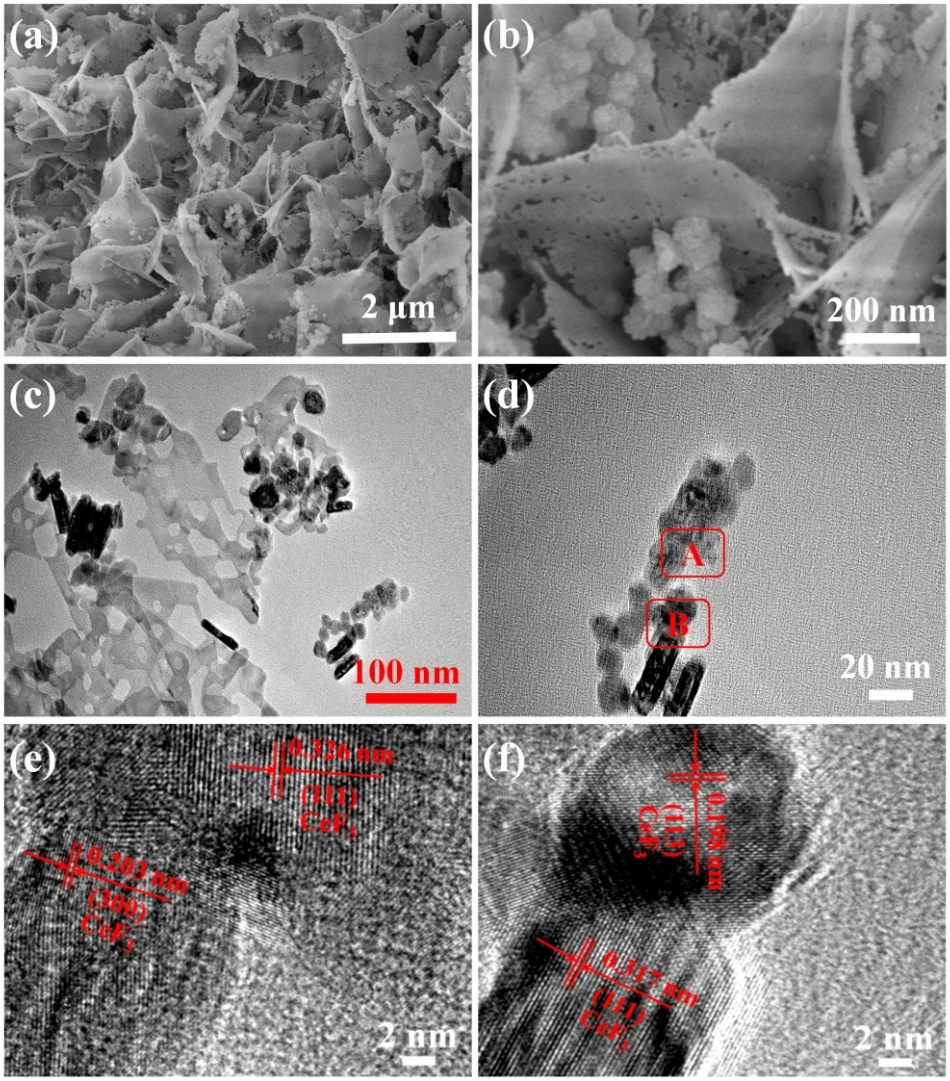

Fig. S8 SEM images of NiO/CeO_2 hybrid NFAs fabricated under high concentration (20 mM) of $Ce(NO_3)_3$ with (a) low and (b) high magnification, (c) TEM image of a single NiO/CeO_2 hybrid nanoflake with CeF_3 nanoparticles, (e) and (f) are HRTEM images at spots A and B in Fig. S8(d).

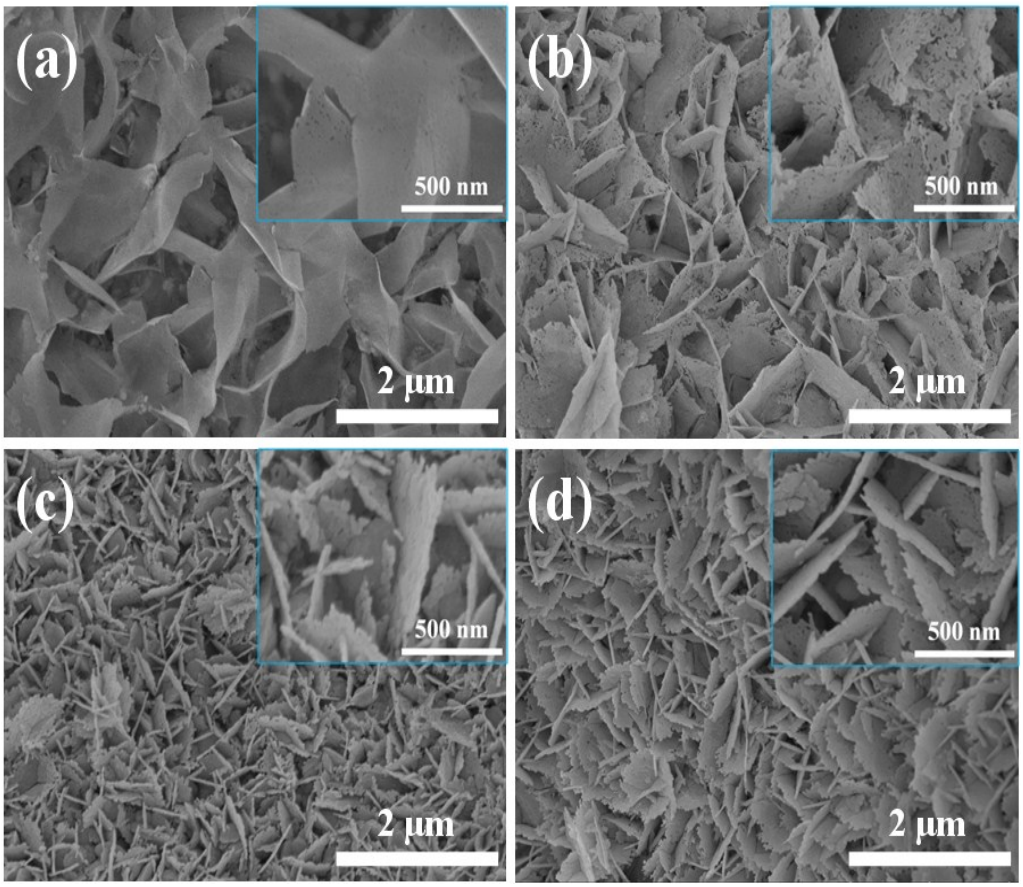

Fig. S9 Influence of hydrothermal temperature on the morphology of NiO/CeO_2 hybrid NFAs. (a) 80℃, (b) 100℃, (c) 120℃ and (d) 140℃.

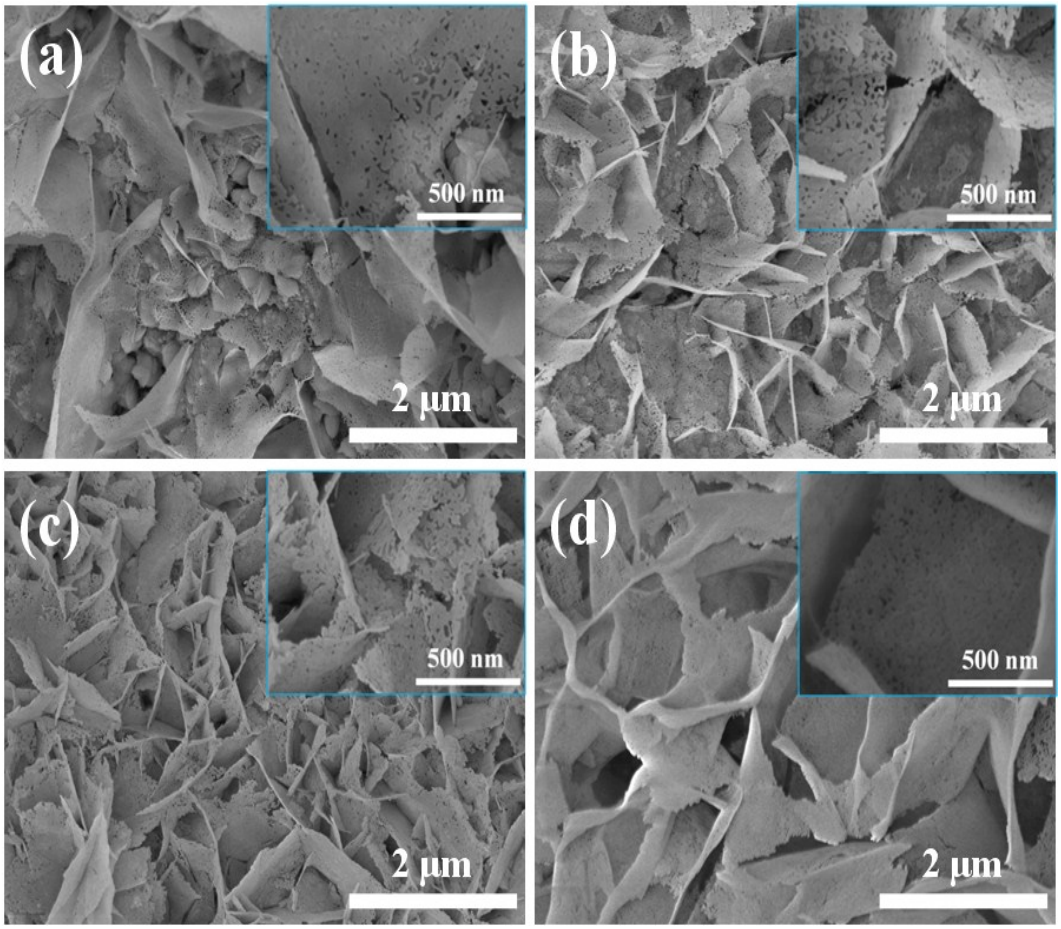

Fig. S10 Influence of hydrothermal time on the morphology of NiO/CeO_2 hybrid NFAs. (a) 4 h, (b) 8 h, (c) 12 h and (d) 16 h.

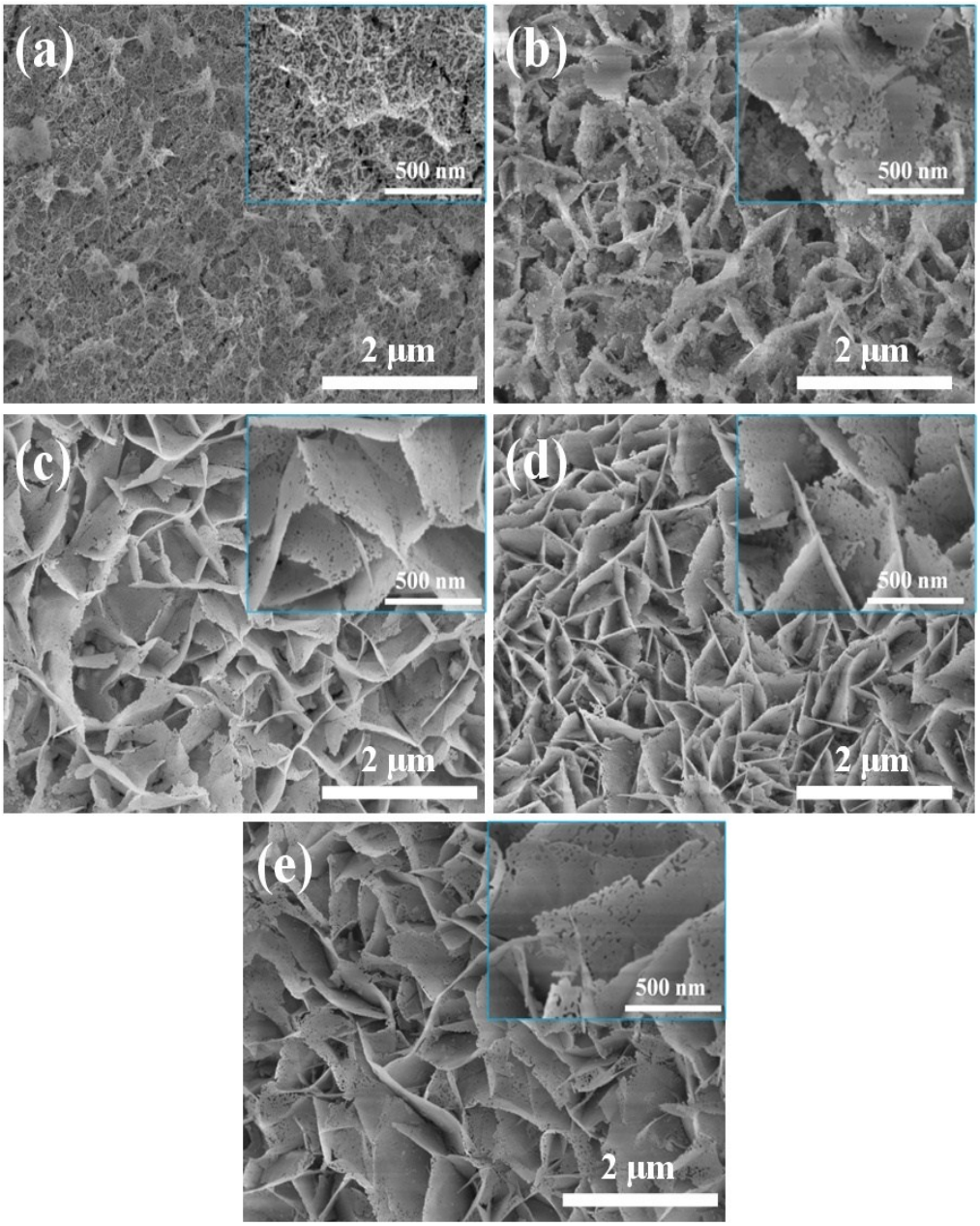

Fig. S11 Influence of NH_4F concentration on the morphology of NiO/CeO_2 hybrid NFAs. (a) 0, (b) 10 mM, (c) 20 mM, (d) 30 mM and (e) 40 mM.

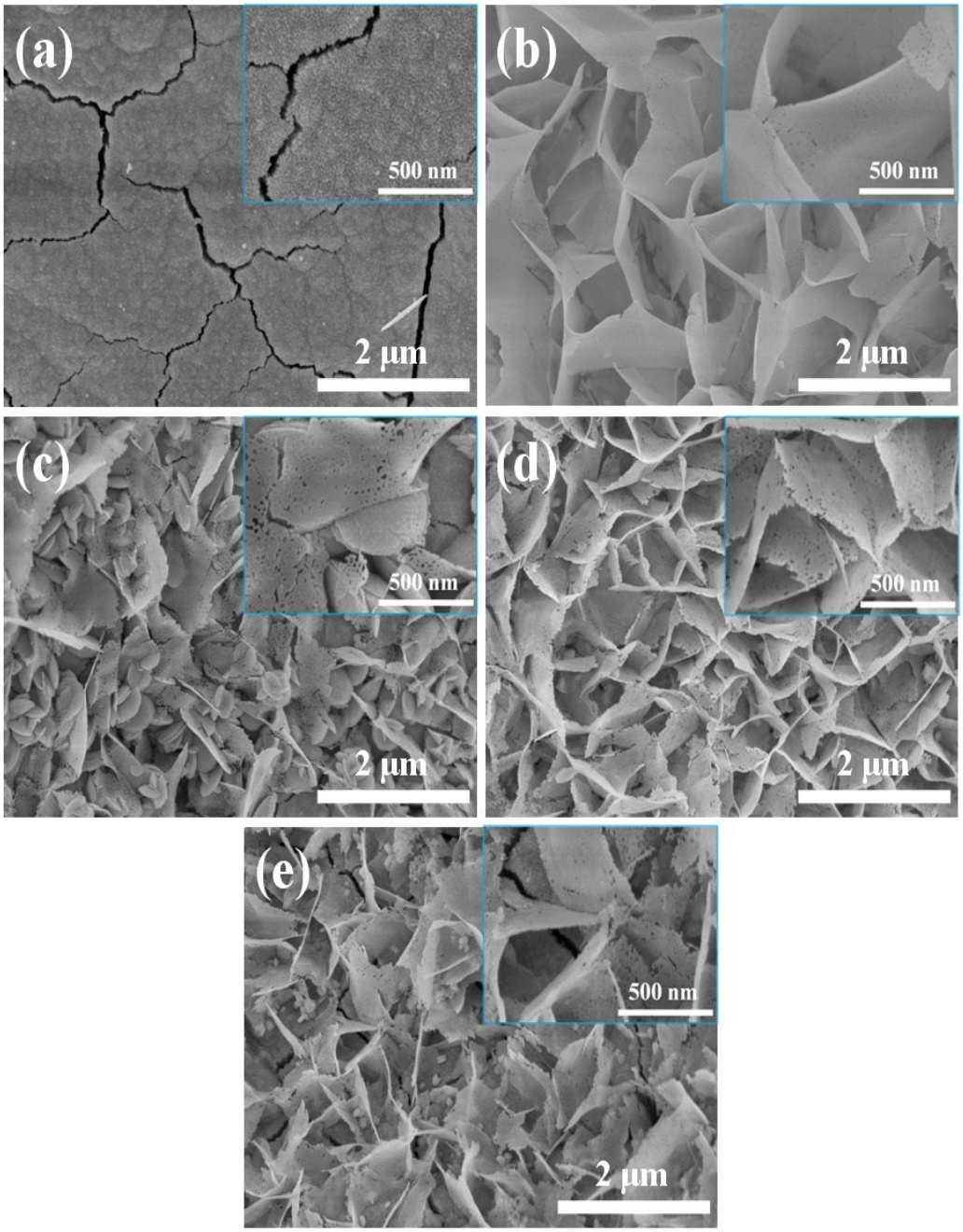

Fig. S12 Influence of $CO(NH)_2$ on the morphology of NiO/CeO_2 hybrid NFAs.
(a) 0, (b) 10 mM, (c) 30 mM, (d) 50 mM and (e)70 mM.

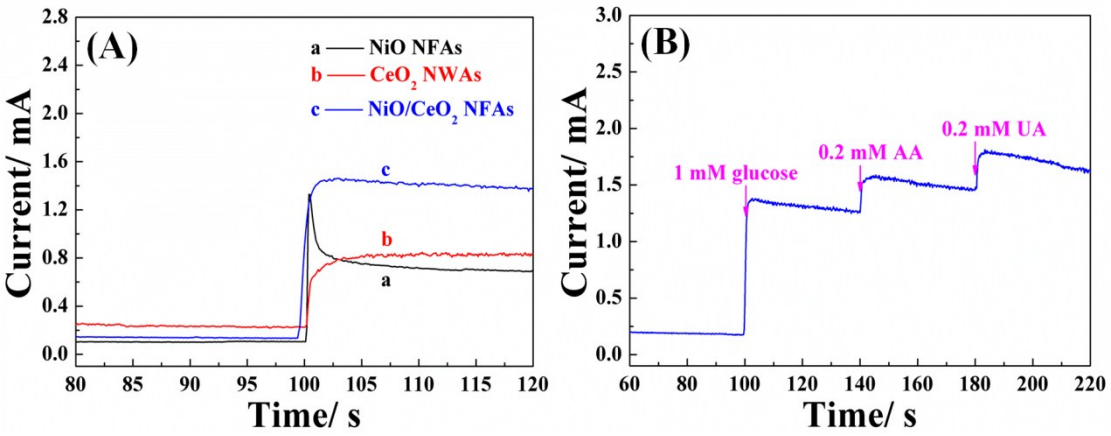

Fig. S13 (A) Amperometric responses of various substrates (a) NiO NFAs, (b) CeO_2 NWAs and (c) NiO/CeO_2 NFAs with injection of 1 mM glucose in 0.1 M NaOH. (B) Anti-interference ability of NiO/CeO_2 NFAs in alkaline solution. Working potential: 0.6 V *vs.* Ag/AgCl.

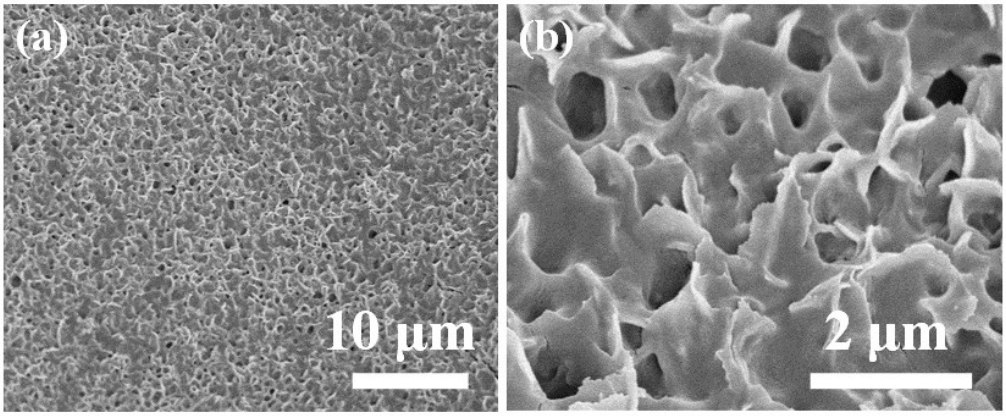

Fig. S14 SEM images of NiO/CeO_2 NFAs after modification with low (a) and high (b) magnification

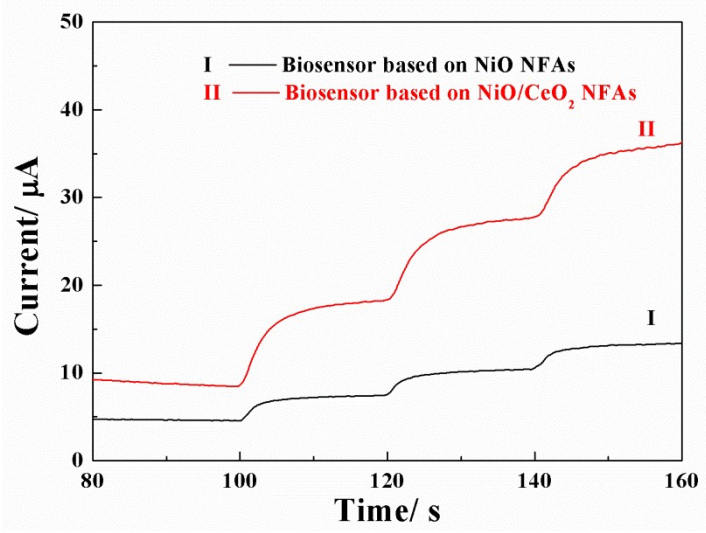

Fig. S15 Typical amperometric responses of glucose biosensors based on NiO and NiO/CeO_2 NFAs measured under the same condition

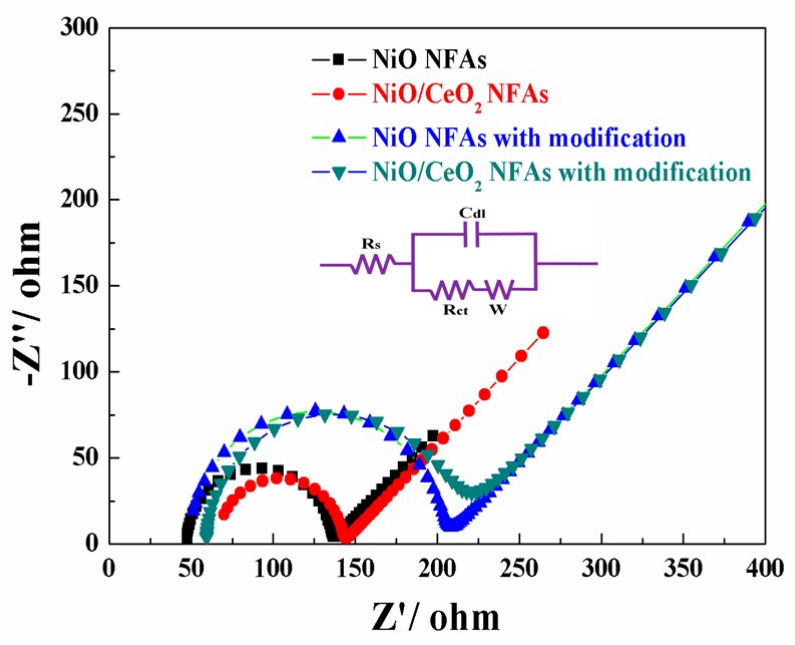

Fig. S16 Nyquist plots of different electrodes in 0.1 M KCl and 5 mM $K_3Fe(CN)_6$. Inset is the equivalent circuit used to fit the experimental data.

Table S2 Fitting parameters based on equivalent electrical circuit shown in the inset of Fig. S15 for different EIS plots

Impedance parameter	R_s/Ω	R_{ct}/Ω	CPE/μF	W/Ω
NiO NFAs	47.46	**87.49**	0.544	0.014
NiO/CeO_2 NFAs	65.87	**76.16**	0.111	0.0073
NiO NFAs with modification	48.77	**153.6**	0.103	0.003
NiO/CeO_2 NFAs with modification	59.19	**146**	0.535	0.0013

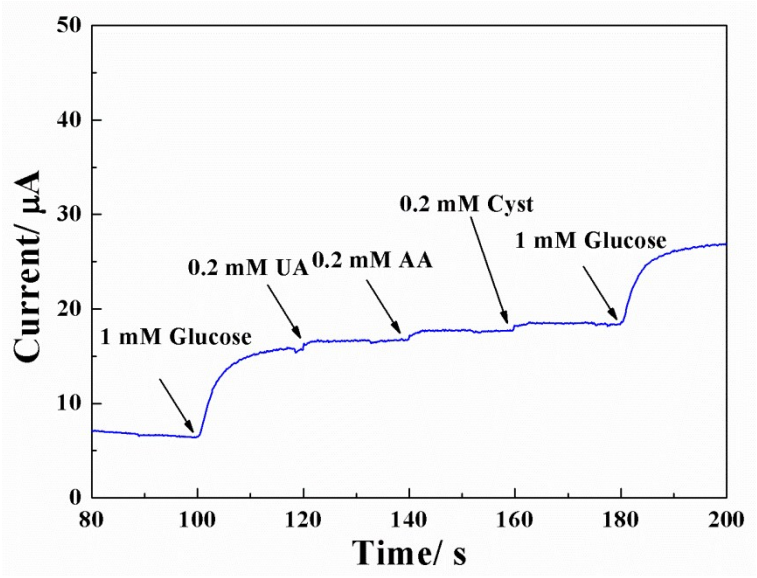

Fig. S17 Anti-interference ability of as-prepared glucose biosensor. Working potential: 0.6 V *vs.* Ag/AgCl.

Table S3 Comparison of glucose biosensors based on NiO/CeO_2 hybrid NWAs and other representative nanomaterials

Electrode materials	Synthesis approach	Sensitivity $\mu A \cdot cm^{-2} \cdot mM^{-1}$	Linear range μM	LOD μM	Working potential V	Ref.
NiO/CeO_2 NWAs	**One-step Hydrothermal**	**154.4**	**1.0-2,900**	**1.0**	**0.6**	Present work
ZnO nanorod array	One-step Hydrothermal	23.1	10-3,450	10	0.8	2
ZnO nanotube array	Two-step electrochemical/chemical process	30.85	10-4,200	10	0.8	3
ZnO nanofiber	Electrospinning technique	70.2	250-19,000	1.0	0.8	4
CeO_2 nanorod	Electrophoretic deposition	0.165	2,000-26,000	100	0.8	5
NiO film	RF sputtering technique	101.8	1,380-16,660	800	/	6
NiO nanosphere	Precipitation method	4.3 $\mu A \cdot mM^{-1}$	1,500-7,000	47	0.35	7
MnO_2	Sol-gel process	24.2	0.9-2,730	0.18	0.6 V	8
NiO/ZnO nanorods	One-step Hydrothermal	61.78	500-8,000	2.5	0.39	9
AuNP/PB/TiO_2 nanotube array	Anodization + photocatalytic deposition	248.0	10-700	3.2	-0.35	10
ssDNA-SWCNT	Layer-by-layer electrostatic self-assembly	6 $nA \cdot mM^{-1}$	Up to 94,000	38	0.5	11
MWCNT	Plasma enhanced chemical vapour deposition	/	Up to 30,000	80	-0.2	12
RGO	Modified Hummer's method	1.85	100-27,000	/	-0.44	13
GR-CNT-ZnO	Modified Hummer's method + Ultrasonication + Reduction	5.36	10-6,500	4.5	/	14
GR-PFIL	Modified Hummer's method + Covalent method	/	2,000-14,000	2,000	/	15
N-doped GR	Modified Hummer's method + Nitrogen Plasma treatment	/	100-1,100	10	-0.15	16

Note:

LOD---Limit of Detection

SWCNT---Single-wall Carbon nanotube

MWCNT---Multi-wall Carbon nanotube

RGO---Reduced Graphene Oxide

GR--- Graphene

PFIL--- Polyethylenimine-Functionalized Ionic Liquid

References:

1. J. W. Cui, S. B. Adeloju, Y. C. Wu, Anal. Chim. Acta, 2014, 809,134.
2. A. Wei, X. Sun, J.X. Wang, Y. Lei, X.P. Cai, C.M. Li, Z. Dong, Appl. Phys. Lett., 2006, 89, 123902.
3. K. Yang, G. W. She, H. Wang, X. M. Ou, X. H. Zhang, C. S. Lee, S. T. Lee,J. Phys. Chem. C, 2009, 113,20169.
4. M. Ahmad, C. F. Pan, Z. X. Luo, J. Zhu,J. Phys. Chem. C, 2010, 114, 9308.
5. D. Patil, N. Q. Dung, H. Jung, S. Y. Ahn, D. M. Jang, D. Kim, Biosens. Bioelectron., 2012, 31, 176-181.
6. M. Tyagi, M. Tomar, V. Gupta, Anal. Chim. Acta, 2012, 726, 93.
7. C. C. Li, Y. L. Liu, L. M. Li, Z. F. Du, S. J. Xu, M. Zhang, X. M. Yin, T. H. Wang, Talanta, 2008, 77, 455.
8. J. J. Yu, T. Zhao, B. Z. Zeng, Electrochem. Commun., 2008, 10, 1318.
9. X. F. Chu, X. H. Zhu, Y. P. Dong, T. Y. Chen, M. F. Ye, W. Q. Sun, J. Electroanal. Chem., 676, 2012, 20.
10. Z. D. Gao, Y. F. Ou, T. T. Li, N. K. Shrestha, Y. Y. Song, Sci. Rep., 2014, 4, 6891.
11. Z. Kang, X. Q. Yan, Y. Zhang, J. Pan, J. Shi, X. H. Zhang, Y. Liu, J. H. Choi, D. M. Porterfield, ACS Appl. Mater. Interfaces, 2014, 6, 3784.
12. Y. H. Lin, F. Lu, Y. Tu, Z. F. Ren, Nano Lett., 2004, 4, 191.
13. B. Unnikrishnan, S. Palanisamy, S. M. Chen, Biosens. Bioelectron., 2013, 39, 70.
14. K. Y. Hwa, B. Subramani, Biosens. Bioelectron.,2014, 62, 127.
15. C. S. Shan, H. F. Yang, J. F. Song, D. X. Han, A. Ivaska, L. Niu, Anal. Chem. 2009, 81, 2378.
16. Y. Wang, Y. Y. Shao, D. W. Matson, J. H. Li, Y. H. Lin, ACS Nano, 2010, 4,1790.